SCIENTIFIC PAPERS
OF THE UNIVERSITY OF PARDUBICE
Series A
Faculty of Chemical Technology
4 (1998)

EFFECTS OF RHEOLOGICAL BEHAVIOUR ON CROSSFLOW MICROFILTRATION OF CONCENTRATED SHEAR-THINNING DISPERSIONS

Petr MIKULÁŠEK
Department of Chemical Engineering, University of Pardubice,
CZ-532 10 Pardubice

Received September 4, 1998

The effect of process variables on permeate flux during the crossflow microfiltration of concentrated titania dispersions has been investigated. Filtration experiments carried out on ceramic, tubular crossflow modules have shown that increases in transmembrane pressure, crossflow velocity and the degree of dispersion flocculation all result in an improved permeate flux. Rheological work has shown that the titania dispersions exhibit shear-thinning behaviour, conforming to the Herschel–Bulkley or the Casson type models in the shear rate range investigated. Extreme sensitivity with pH was observed, whereby the dispersion viscosity can be changed by as much as an order of magnitude with pH variation at constant volume fraction. The effects of both shear rate and pH are enhanced as the dispersion concentration is increased and the iso-electric point approached. These observations have important implications in crossflow microfiltration of these dispersions.

Introduction

Cross-flow membrane microfiltration is a separation process for removal of dispersed matter with particles ranging from 0.05 to 10 μm from a liquid stream by forcing the liquid to pass through a porous membrane. As opposed to dead-end microfiltration, where the dispersion is forced normal to the membrane, the dispersion in cross-flow filtration is forced tangential to the membrane surface. This generates a number of forces which tend to remove the deposited layers from the membrane surface thus helping to keep the membrane relatively clean. The main applications of this process are in the production of ultrapure water, the processing of food and dairy products, the recovery of electrodeposition paints, the treatment of oil and latex emulsions and in biotechnology-oriented applications such as fractionation of fermentation broths and high performance reactors for enzymatic and fermentation processes. Crossflow microfiltration of dispersions is encountered in a wide variety of engineering applications, such as solid-liquid separation, water purification, and drilling operations. The primary focus of our study is the crossflow microfiltration of concentrated dispersions of titanium dioxide in water. These concentrated dispersions arise in various industrial applications such as paints, coatings, and joint treatment compounds. These systems typically exhibit complex rheological behaviour [1,2].

Models based on the theory of fouling phenomena and concentration polarisation and hydrodynamic models have been developed to predict the steady-state permeate flux of crossflow microfiltration (see, for example, Refs [3–5]). These models can be loosely categorised as being either based on a film theory, following a development based on convection of matter towards the membrane and diffusion of the retained species back into the crossflow, possibly incorporating lift forces, or cake theory which applies Darcy's law to relate filtration rate to average pressure difference between inside the filter and the permeate line. However, the applicability of these models over a wide range of operating conditions including temperature, crossflow velocity, pressure drop, particle size, particle concentration in the dispersion, pH, and electrolyte concentration is in doubt because they do not consider the influence of all of the significant terms and their outeractions. For any model to be realistic it must be able to show the effects of the dispersion viscosity and particle-particle interactions, which may have hydrodynamic or nonhydrodynamic origins. The qualitative difference in the crossflow microfiltration behaviour of non-Newtonian dispersions under constant tangential feed and constant inlet pressure conditions, shown, for example, by Vassilieff et al. [6] and Marchant and Wakeman [7,8], are not consistent with the predictions of these models.

The rheological properties of dispersions are governed by the microstructure of the system. In these systems, the solid particles are relatively small and the interparticle forces are significantly pronounced so as to influence the microstructure, the state of aggregation of the dispersion and, consequently, the

mechanical and rheological properties of the system. Thus, it is of interest to study the rheological behaviour of these systems in order to understand and control the flow behaviour and stability of these materials.

In the present article, crossflow filtration experiments have been performed on aqueous dispersions of titanium dioxide through a tubular ceramic membrane. The feed concentration, flow rate and transmembrane pressure were varied. The focus is on analysing the effects of pH and the relative contribution of the rheology on the transient flux decline and the steady-state flux during microfiltration of concentrated titanium dioxide dispersions.

Experimental

Materials

The titanium dioxide used was rutile supplied by Tioxide Group Ltd., England. Rutile (density: 4 260 kg m $^{-3}$) has a higher refractive index, higher density and greater chemical stability than anatase. The crystal size for rutile TiO_2 pigments, which is different from particle size (0.25 – 0.40 μm), is 0.17 – 0.24 μm. Transmission electron microscopy was used to estimate the shape and aspect ratio of the rutile crystals, which were found to be approximately elliptic and 2 – 3, respectively. The particle size distributions were measured using a MasterSizer MS20 (Malvern Instruments Ltd., England).

The dispersions were prepared by mixing the appropriate amount of Millipore-filtered water and the titanium dioxide in a high shear, Ultra-Turrax T25, mixer (Janke & Kunkel, IKA-Labortechnik, Germany), with the help of a dispersant CALGON (sodium hexametaphosphate). The samples prepared contained 0.15% by weight of dispersant. Whereas the volume percent of solids was varied, the mass of dispersant per unit mass of solids was kept constant. This was to ensure that there was always an adequate amount of dispersant available for steric stabilisation.

Zeta potential measurements to get information on the state of charge at the solid-liquid interface were carried out by means of a microelectrophoresis device (Zetasizer 3, Malvern Instruments Ltd., England).

The pH value of the system was adjusted by adding various amounts of HCl or NaOH into deionised water, which was used as the suspending medium. All the reagents of soluble acid and alkali used were analytical grade. The pH was measured with a pH Meter Model 80 (Griffin & George Ltd., England). The dispersion was stirred until a steady pH reading was obtained.

Rheological Measurements

A Carri-Med Model CS 100 controlled stress rheometer, either with double concentric or cone and plate system, was used for the steady shear measurements. However, the cone and plate system has been used for the highest volumetric concentrations of solids in the samples (50 vol.%) only. The temperature of the samples was controlled by a Peltier system. All measurements except those of the temperature effect study were conducted under ambient conditions (T = 20 °C). Measurements of the effect of temperature were conducted for temperatures ranging from ambient to 50 °C. The temperature was maintained to within ±0.1 °C of the desired pre-set value. Water evaporation was potentially a serious problem when the experiment was performed above 30 °C. Therefore, the interface exposed to the atmosphere was coated with a thin layer of silicone oil to minimize evaporation. The rheological measurements suggested the use of a model of the Herschel–Bulkley type

$$\tau = \tau_{HB} + K\dot{\gamma}^n \tag{1}$$

or of the Casson type

$$\tau^{1/2} = \tau_C^{1/2} + (\eta_\infty \dot{\gamma})^{1/2} \tag{2}$$

to characterize the rheological behaviour of these dispersions [9]. The existence of a yield stress has been observed, especially at the highest volumetric concentrations of solids. In addition, it should be noted that a positive value for the hysteresis loop area has been obtained and this indicates that the samples with the highest concentrations of the solids exhibited some thixotropy.

Filtration Experiments

Membranes

The ceramic membranes studied in this work were asymmetric, double-layered, silicon carbide (SiC) membranes (Atech Innovations, Germany). They were configured as single cylindrical tubes 0.9 m long, 16 mm ID and 25 mm OD, consisting of a thin SiC layer deposited on the internal surface of the tubular support. In our experiments, the microfiltration membranes were used with the mean pore diameter equal to 0.1 μm.

Equipment

A schematic diagram of the experimental apparatus is shown in Fig. 1. The dispersion is fed to the filter by a variable speed monopump, thus allowing a range of crossflow velocities to be examined. Pressure transducers at either end of the filter module measure the transmembrane pressure, which is controlled using full flow ball valves. Temperatures are monitored by thermocouples, computer controlled, and maintained by a hot water jacket around the feed tank. An automatic data logging system records transmembrane pressure, temperature, and pump speed while permeate flux measurements are taken manually.

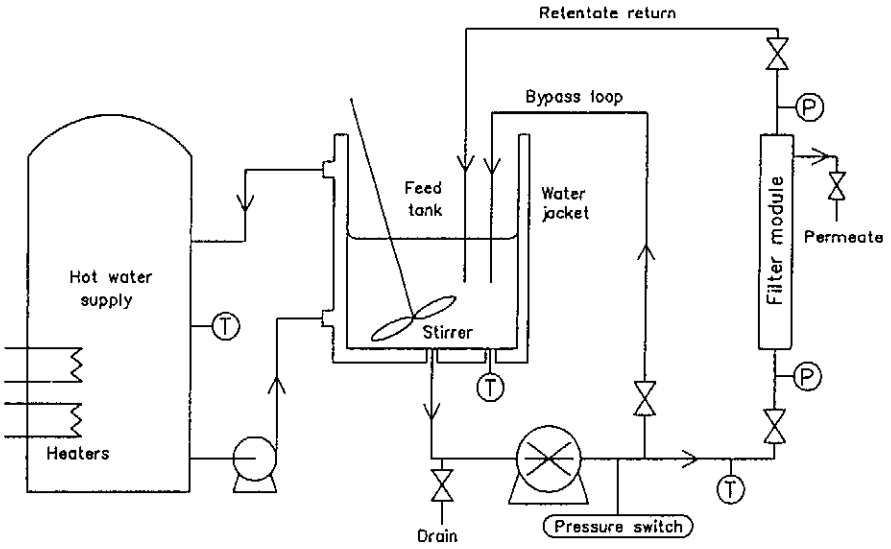

Fig. 1 Schematic diagram of crossflow microfiltration rig

Once the dispersion is circulating through the bypass loop at the required volumetric flow rate, concentration, pH, and temperature, the valve to the filter module is opened and the bypass loop closed. The filter module exit valve is then adjusted to achieve the desired transmembrane pressure, whereupon permeate flux readings are taken and the flux decline is monitored until a steady-state is reached.

Experiments were carried out at 50 °C. The permeate flux, J, for various inlet crossflow velocities in the range of 0.3 – 2 m s^{-1} and various transmembrane pressures in the range of 50 – 200 kPa, was evaluated. The same membrane was used in each experiment, and before the run, the pure water flux through the membrane was measured. The flux through the membrane was measured by collecting the permeate from the outer stainless steel tube surrounding the membrane into graduated cylinder and timing the collection period. Both the permeate and the

retentate were recycled to the storage tank. Therefore, the concentration in the container remained virtually constant. The unit allowed studies in which the transmembrane pressure and the cross-flow velocity were independently varied. By systematically adjusting one process variable whilst maintaining all others constant, steady-state permeate flux values were obtained as a function of each variable.

Results and Discussion

Viscosity Measurements

The results of the viscosity measurements are presented in Fig. 2 showing a pronounced non-Newtonian behaviour of the aqueous titania dispersions (in agreement with the data presented in Ref. [2]). The pronounced shear-thinning rheological behaviour can be approximated with a model of the Herschel– Bulkley type or of the Casson type. For the former, Table I gives the values obtained for the various parameters as functions of the volume fraction of solids.

The variation of the yield stress as a function of the volume fraction of solids shows that neither τ_{HB} nor τ_C increases strongly above the concentration of 10

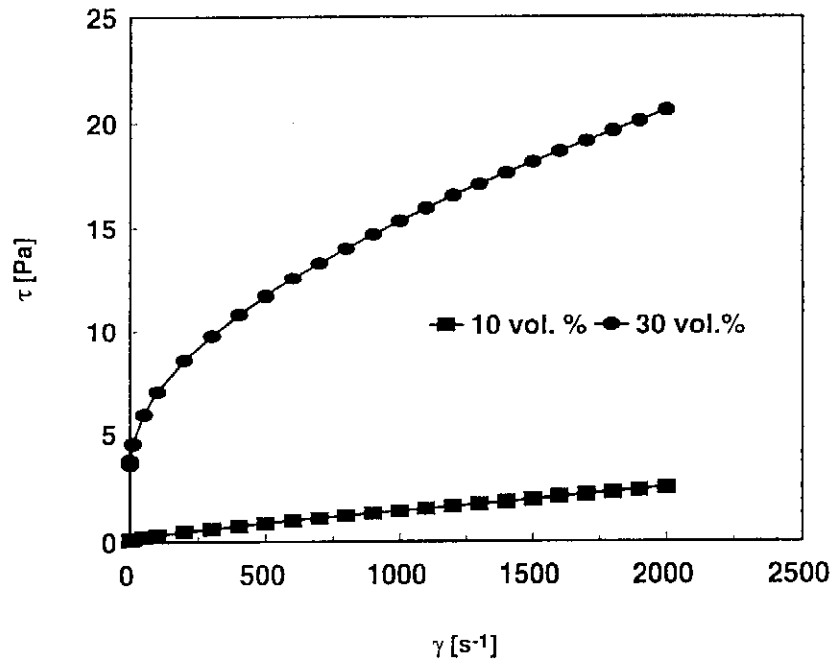

Fig. 2 Rheogram of the shear stress against the shear rate for 10 and 30 vol.% titanium dioxide dispersions at pH 9.5 and temperature 50 °C.

vol.%. The values of the yield stresses, calculated on the basis of the two rheological models, are very close to one another for the volume fractions above 10% (the differences between the two values fall between 2 and 5%). The percentile difference is considerably larger for lower concentration.

Tab. I Parameters of the Herschel–Bulkley model as a function of the solids volume fraction of aqueous titania dispersions (T = 50 °C, pH 9.5).

φ	τ_{HB}, Pa	K, Pa s^n	n
0	0	5.494×10^{-4}	1
0.05	0.0106	1.519×10^{-3}	0.919
0.10	0.1592	4.468×10^{-3}	0.834
0.20	1.459	0.1041	0.676
0.30	3.517	0.2982	0.529
0.40	10.99	0.6232	0.487
0.50	25.52	1.108	0.448

The consistency, K, of the Herschel–Bulkley model also increases strongly above this critical volume fraction of 10%. In addition, the curve for the variation of the flow index, n, of the dispersion shows clearly that there is a change in the rheological behaviour of the titania dispersions when the volume fraction of solids exceeds 30%.

The effect of pH on the rheological properties of a 10 vol.% titanium dioxide/water dispersions is shown in Fig. 3. The results in Fig. 3 show that the dispersions are shear-thinning and are characterised by a non-linear flow curve which asymptotes at low shear rate to the yield stress of the dispersion. The position of the shear-thinning flow curves is pH dependent. This is due to the different degree of flocculation in the dispersion at different pH values.

Figure 4 shows the effect of pH on the apparent viscosity of 1, 10, 30, and 50 vol.% titanium dioxide dispersions. The viscosity was evaluated at the shear rate of 500 s^{-1}. On the basic side (pH: 7 – 14), the viscosity first decreases with pH, reaching a minimum near pH 9, and then increases as the pH becomes higher. The low apparent viscosity behaviour is a strong indication that the systems are dispersed. On the acidic side (pH: 7 – 0), the same trend is observed. As the pH decreases (i.e. through the addition of more HCl) the ionic strength is raised. This can lead to a decrease of the electrical double layer repulsion and flocculation occurs due to van der Waals attractions. The high viscosity behaviour at pH 4, as observed in Fig. 4, may be explained by this ionic strength effect. The pH value at maximum viscosity should correspond to the isoelectric point of the titanium di-

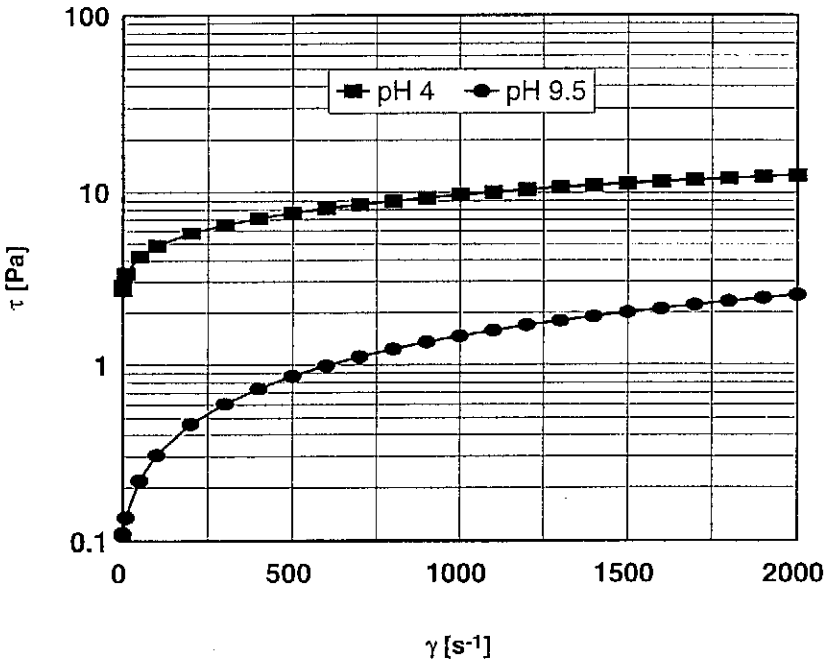

Fig. 3 Effect of pH on the flow properties of 10 vol.% titanium dioxide dispersions at temperature 50 °C.

oxide. The isoelectric point is the pH at which the electrophoretic mobility is zero, which occurs when there is no net surface charge on the colloidal particle. At pH below the isoelectric point, the surface charge for most metallic oxides such as alumina, titania, zirconia, is positive which is attributed to the protonation of the surface hydroxyl group [10].

In order to verify the effect of pH on the system behaviour, the zeta (ζ) potential vs pH relationship was measured and is shown in Fig. 5. At pH 4.0 the ζ-potential was 4.4 mV, at pH 6.8 (the natural pH of the dispersion approximately) it was −43.6 mV, and at pH 9.4 it was −51.4 mV. The isoelectric point, or the point of zero electrophoretic mobility, is at pH 4.2. This value agrees well with a value of 4 from the viscosity measurements and a value of about 5 obtained from particle size measurements (see Fig. 5). The electrophoretic mobility parametr, which is a measure of the velocity of a charged particle in an electric field, is dependent on the ionic strength, the presence of dispersant, and the presence of an inorganic coating on the titanium dioxide particles. Since impurities are difficult to eliminate completely, it is common to find a range in the isoelectric point values quoted for the same material in the literature. A literature survey reveals that the isoelectric point reported for titanium dioxide varies from pH of 4.0 to 6.1 (Refs [10–12]).

One of the properties of the particles which will vary with pH is their size

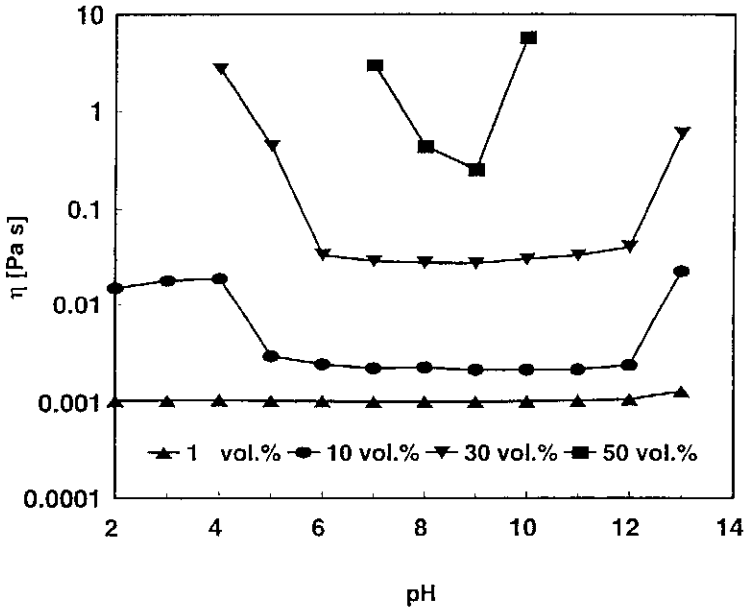

Fig. 4 Effect of pH on the apparent viscosity (evaluated at 500 s^{-1}) of 1, 10, 30, and 50 vol.% titanium dioxide dispersions

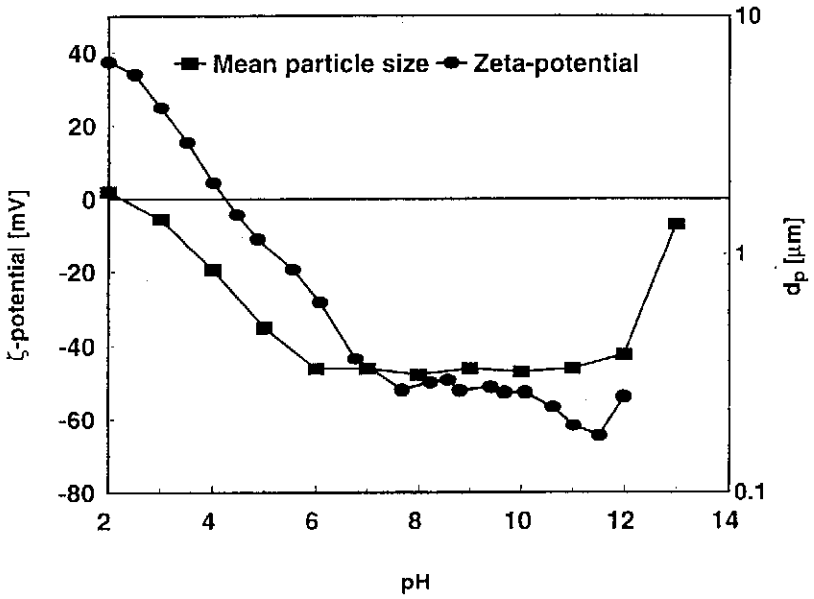

Fig. 5 The variation of zeta-potential and mean particle diameter with pH for rutile (titanium dioxide) used in the experiments

distribution. The size distribution of the dispersions at pH values of 2.0, 4.0 and 9.5 is shown in Fig. 6. At pH 9.5 the particles have a relatively narrow size distribution with a mean size of 0.35 μm. As the pH is decreased flocculation becomes progressively more important, the peak in the size distribution of the flocs occurring at 1.5 – 2.5 μm.

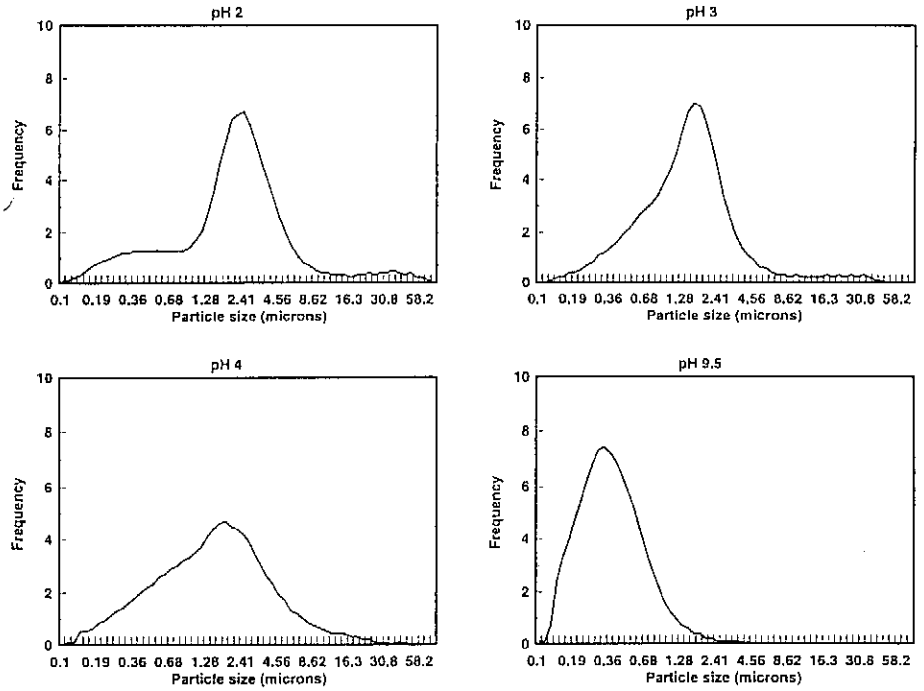

Fig. 6 Variation of the size distribution of titanium dioxide dispersions with pH

A plot of the variation of the apparent viscosity (evaluated at 500 s^{-1}) as a function of the volumetric concentration of solids and pH (Fig. 7) shows that the viscosity increases strongly above the concentration of 10 vol.% and depends on the pH of the dispersions. The results in Fig. 7 also show that the difference in viscosity between the different states of flocculation or dispersion can be very large. For example, one order of magnitude difference in viscosity is observed between the flocculated 10 vol.% dispersion at pH 4 and the dispersed state of the system at pH 9. The apparent viscosity is about 2.2 mPa s for the dispersed 10 vol.% dispersion and 19 mPa s for the flocculated dispersion at pH 4.

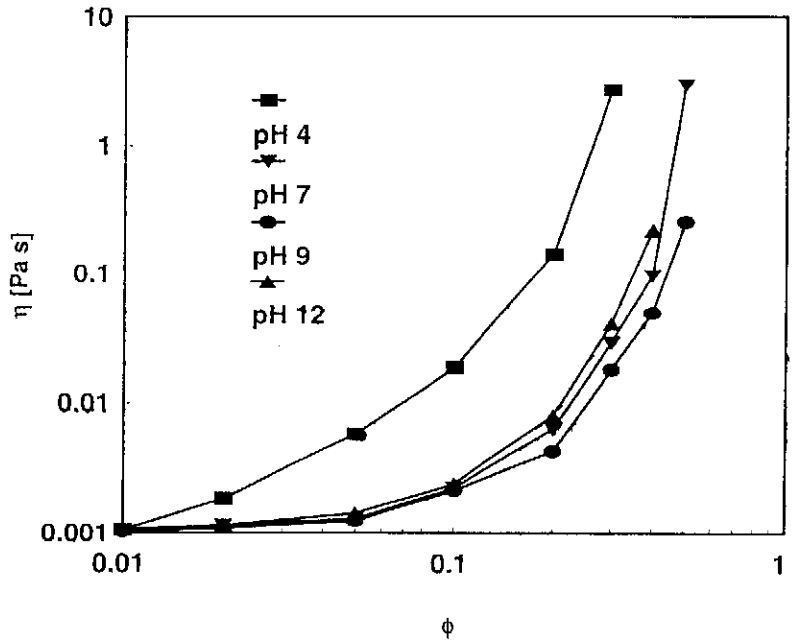

Fig. 7 Variation of apparent viscosity (evaluated at 500 s^{-1}) with the concentration of titanium dioxide dispersions used

Typical Flux Decline Curves

The effect of inlet crossflow velocity, u and bulk dispersion solids volume fraction, φ, on the permeate flux-time curve are depicted in Figs. 8 and 9. As a general rule, the steady-state flux during crossflow microfiltration was substantially lower than the pure water flux ranging from 1% to 10% of the pure water values. Besides the fact that low levels of permeate flux were achieved (for comparison see Refs [13,14]), the most noticeable feature in Figs 8 and 9 is the strong dependence of the flux on the operating variables. The following trends are evident:

a) A significant flux decay was observed mainly in the initial periods of the process, and
b) the flux decline shows significant dependence on operating conditions such as inlet velocity and bulk dispersion solids volume fraction.

The flux decay in the initial periods of the process could be explained by build-up of concentration polarisation and the formation of a cake layer on the membrane surface which offers the controlling hydraulic resistance to permeation. Steady-state conditions as a result of concentration polarisation and the hydraulic

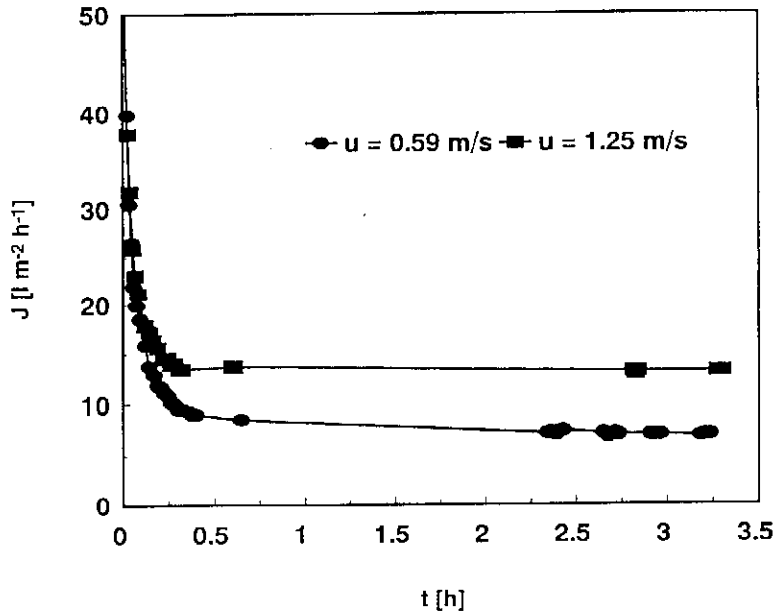

Fig. 8 Effect of inlet velocity on flux-time curve (φ = 0.19, ΔP = 100 kPa)

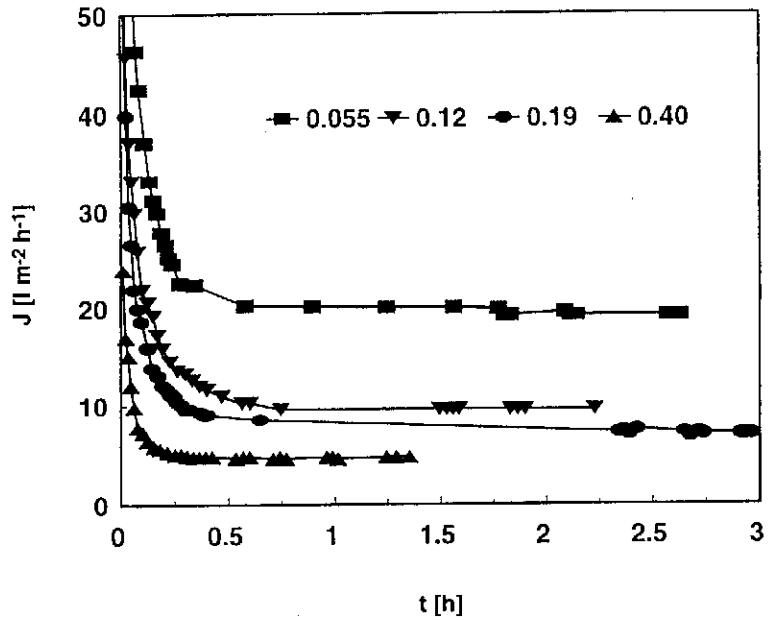

Fig. 9 Effect of bulk solids volume fraction on flux-time curve (u = 0.7 m s^{-1}, ΔP = 100 kPa)

resistance of a cake layer are reached when the convective transport of particles to the membrane is equal to the sum of the permeate flow plus the diffusive back transport of the particle. In addition, the filter cake continues to grow until it reaches a state where further growth is curtailed by the applied axial fluid shear upon the cake layer. At this point, a steady-state flux should be reached.

The effects of the operating variables on the steady-state flux are shown in Fig. 10. The steady-state flux is a strong function of the operating variables investigated. From Fig. 10 it is evident that the steady-state flux increases (the thickness of the cake layer and its hydraulic resistance decreases) with the superficial velocity. Similar trends were observed before [14, 16–18]. Increasing the crossflow velocity of the dispersion increases the shear effect on the filter cake surface. This helps to limit the thickness of filter cake formed, but may also serve to agitate particles in the cake surface layer, resulting in cake consolidation and therefore an increased resistance to permeate flow [19,20]. Figure 10 shows a significant increase in permeate flux with crossflow velocity, suggesting also that the shear effect is limiting the thickness of cake layer formed.

The effects of increasing dispersion concentration on permeate flux can be seen in Fig. 10. At higher concentrations, the relatively high initial flux of particles to the filter surface results in the rapid deposition of a cake layer, minimizing the

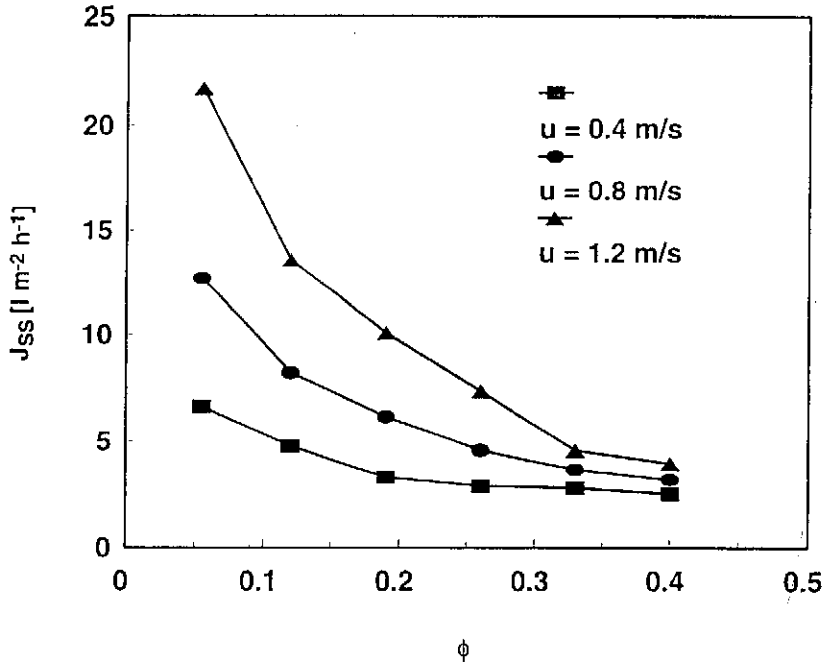

Fig.10 Effect of inlet velocity and bulk solids volume fraction on the steady-state flux

tendencies of particle penetration into the membrane pores and resulting in a more immediate decline in permeate flux. At steady state, the higher concentration results in a thicker filter cake and consequently a lower permeate flux. Additionally, the effects of pH, crossflow velocity and transmembrane pressure on permeate flux are all more pronounced at low concentrations and have a reduced effect at higher concentrations [7,8]. The highest concentration reached during filtration was 48% solids by volume (pH 9.5, 50 °C, 100 kPa, 1.3 $m\,s^{-1}$).

The permeate flux through an unfouled membrane is proportional to the transmembrane pressure and depends little on crossflow velocity. A compressible cake, however, may yield to increased pressure, thus reducing permeate flux. Figure 11 shows an increase in permeate flux with pressure, but a doubling of the flux does not occur when the transmembrane pressure is doubled. This may be due to partial blocking of entrances to the pores in the membrane, as the cake formed is considered to be incompressible.

Figure 12 shows that the permeate flux achieved by filtering a dispersion at pH 4 is much greater than that obtained at pH 9.5. This can be explained by the degree of agglomeration at pH 4 (see Figs 5 and 6) compared to the well dispersed particles of the dispersion at pH 9.5. A filter cake composed of larger aggregates will have a much higher porosity than one of smaller particles, thus providing less

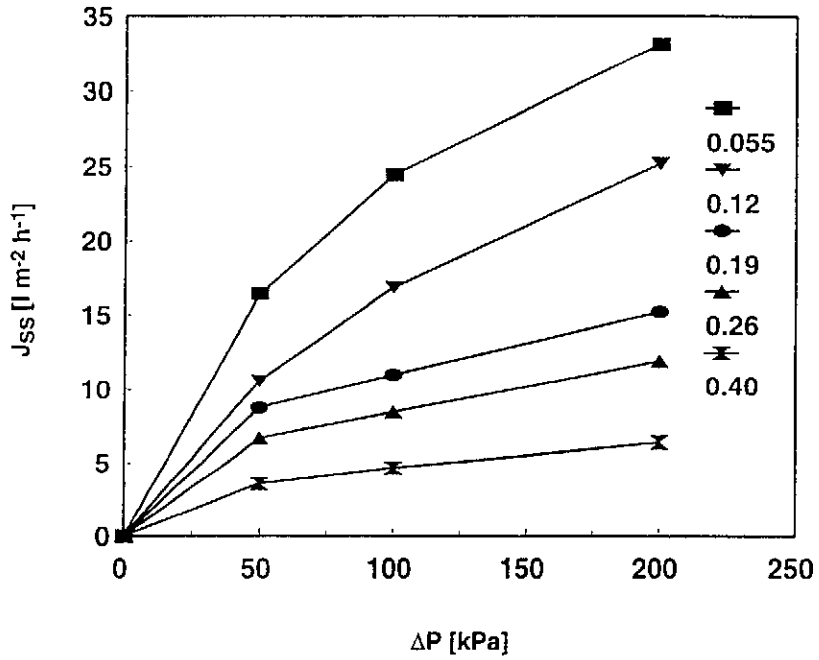

Fig.11 Effect of transmembrane pressure and bulk solids volume fraction on steady-state flux (u = 1.0 $m\,s^{-1}$, pH 9.5)

resistance to the permeate flow.

Clearly, the effects of operating variables on flux differ from system to system. The only general conclusion that may be drawn is that the permeate flux increases with operating velocity and decreases with increasing dispersion concentration. This probably explains why models developed for a particular system may often contradict experimental observations obtained on different systems (see, for example, Refs [3–5]).

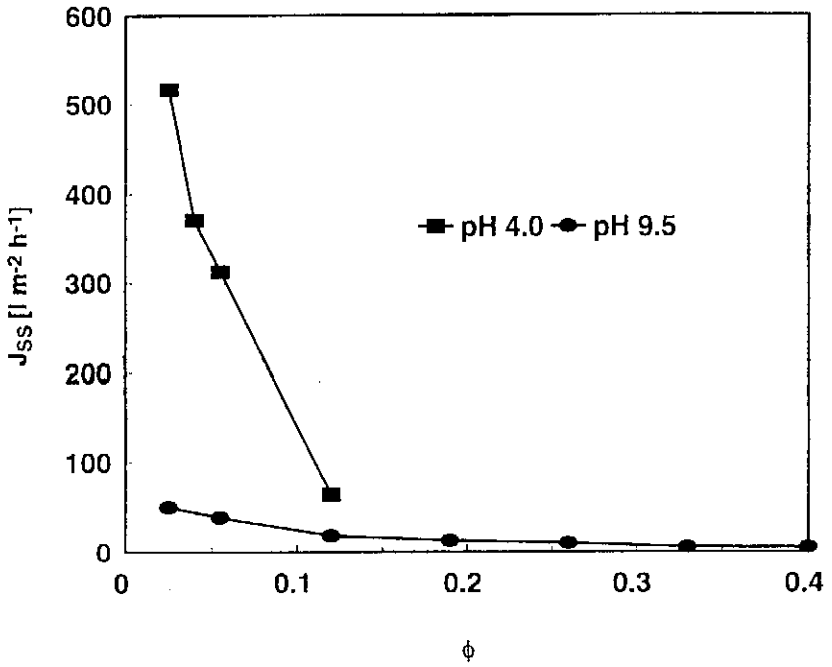

Fig.12 Effect of pH and bulk solids volume fraction on steady-state flux (u = 1.3 m s^{-1}, ΔP = 100 kPa)

Conclusion

The rheological characterisation has revealed that the titania dispersion has a peak viscosity around the iso-electric point (pH 4.0), at which point the effective mean particle size is also at its maximum. The dispersions are shear-thinning and thus become less viscous as shear rate is increased, also becoming more viscous with increasing solids fraction.

The characteristic permeate flux-time behaviour and effects of operating variables on flux data have been presented for aqueous titanium dioxide dispersions that were crossflow microfiltered in a ceramic membrane tube. The flux-time curve,

and the steady-state permeate flux, are functions of all the operating variables studied, i.e. inlet crossflow velocity of bulk dispersion, bulk solids volume fraction and transmembrane pressure difference.

Results of crossflow experiments have revealed a decrease in permeate flux with an increased solids concentration, a lower crossflow velocity and a smaller transmembrane pressure. The cake appears to be incompressible and tends to consolidate further with increasing crossflow velocity. There is also a significant increase in permeate flux when the pH is close to the iso-electric point.

Acknowledgements

The author is grateful to The Royal Society Postdoctoral Fellowship Programme which supported his stay at Department of Chemical Engineering, Loughborough University, UK.

Symbols

d_p	particle diameter, m
J	permeate flux, $l\,m^2\,h^{-1}$
J_{SS}	steady-state permeate flux, $l\,m^2\,h^{-1}$
K	consistency parameter, $Pa\,s^n$
n	flow index
ΔP	transmembrane pressure, Pa
t	time, s
u	inlet crossflow velocity of bulk dispersion, $m\,s^{-1}$
γ	shear rate, s^{-1}
η	apparent viscosity, Pa s
η_∞	constant viscosity at the infinite shear limit, Pa s
τ	shear stress, Pa
τ_C	yield stress in the Casson model, Pa
τ_{HB}	yield stress in the Herschel–Bulkley model, Pa
φ	solids volume fraction

References

1. Jones D.A.R., Leary B., Boger D.V.: J. Colloid Interface Sci. **147**, 479 (1991).
2. Mikulášek P., Wakeman R.J., Marchant J.Q.: Chem. Eng. J. **67**, 97 (1997).
3. Davis R.H.: Sep. Purif. Methods **21**, 75 (1992).
4. Davis R.H.: *Theory for Crossflow Microfiltration, Membrane Handbook,*

(W.S. Winston Ho, K.K. Sirkar, eds), p. 480, Van Nostrand Reinhold, New York 1992.
5. Belfort G., Davis R.H., Zydney A.L.: J. Membr. Sci. **96**, 1 (1994).
6. Vassilieff C.S., Momtchilova I.G., Krustev R.A.: Colloids Surf. A **92**, 231 (1994).
7. Marchant J.Q., Wakeman R.J.: *Crossflow microfiltration of concentrated suspensions*, Research poster meeting "The processing of soft solids and particle technology", Loughborough University 1997.
8. Marchant J.Q., Wakeman R.J.: *Crossflow microfiltration of concentrated titania suspensions*, Proc. IChemE Jubilee Research Event, Vol. 2, p. 1061, Nottingham 1997.
9. Nguyen Q.D., Boger D.V.: Annual Rev. Fluid Mech. **24**, 47 (1992).
10. Leong Y.K., Boger D.V., Parris D.: Trans IChem. **69A**, 381 (1991).
11. Strauss H., Heegn H., Strienitz I.: Chem. Eng. Sci. **48**, 323 (1993).
12. Bowen W.R., Goenaga X.: I.Chem.E. Symp. Ser. **118**, 107 (1990).
13. Hunter R.: *Foundations of Colloid Science, Vol. I,* Oxford Science Publications, Oxford 1987.
14. Asaadi M., White D.A.: Chem. Eng. J. **48**, 11 (1992).
15. Holdich R.G., Cumming I.W., Ismail B.: Trans IChem. **73A**, 20 (1995).
16. Rautenbach R., Schock G.: J. Membr. Sci. **30**, 231 (1988).
17. Schulz G., Ripperger S.: J. Membr. Sci. **40**, 173 (1989).
18. Wakeman R.J.: Trans. IChemE. **72A**, 530 (1994).
19. Tarleton E.S., Wakeman R.J.: Trans. IChemE. **72A**, 431 (1994).
20. Fane A.G.: J. Membr. Sci. **20**, 249 (1984).